Long-lasting molecular alignment: Fact or fiction?

Juan Ortigoso,[1,a)] Mirta Rodríguez,[1] Julio Santos,[1] Attila Karpati,[2] and Viktor Szalay[2]
[1]*Instituto de Estructura de la Materia, CSIC, Serrano 121, 28006 Madrid, Spain*
[2]*Research Institute for Solid State Physics and Optics, Hungary Academy of Sciences,*
P.O. Box 49, H-1525 Budapest, Hungary

It has been suggested that appropriate periodic sequences of laser pulses can maintain molecular alignment for arbitrarily long times [J. Ortigoso, Phys. Rev. Lett. **93**, 073001 (2004)]. These aligned states are found among the cyclic eigenstates of truncated matrix representations of the one-period time propagator $U(T,0)$. However, long time localization of periodic driven systems depends on the nature of the spectrum of their exact propagator; if it is continuous, eigenstates of finite-basis propagators cease to be cyclic, in the long time limit, under the exact time evolution. We show that, for very weak laser intensities, the evolution operator of the system has a point spectrum for most laser frequencies, but for the laser powers needed to create aligned wave packets it is unknown if $U(T,0)$ has a point spectrum or a singular continuous spectrum. For this regime, we obtain error bounds on the exact time evolution of rotational wave packets that allow us to determine that truncated aligned cyclic states do not lose their alignment for millions of rotational periods when they evolve under the action of the exact time propagator. © *2010 American Institute of Physics*.
[doi:10.1063/1.3312533]

I. INTRODUCTION

In the last years, time-dependent phenomena are becoming a central topic of research in atomic and molecular physics. Some important examples are related to quantum control processes for Bose–Einstein condensation,[1] Rydberg atoms,[2] or molecular alignment and orientation.[3] These processes involve atoms or molecules driven by time-dependent external fields, for which theoretical and computational treatments based on Floquet theory are increasingly used. These works usually mention some concern about the convergence properties of finite matrix representations of one-period time propagators, also called Floquet operators, but apart from a paper by Hone *et al.*,[4] this problem has not received much attention in the chemical physics literature. Basically, it is assumed that good convergence can be obtained by increasing the size of the basis set, but this is true only when the Floquet operator has a point spectrum, which may not always be the case.

It has been suggested in previous works[5,6] that for a molecule interacting with a periodic train of nonresonant laser pulses rotational wave packets can exist for which strong alignment is maintained during a long sequence of pulses. These wave packets are cyclic states in the sense that the initial state is reassembled at the end of each laser pulse. Approximate cyclic aligned states were obtained in Ref. 5 and our primary interest here is to determine whether they remain cyclic under the action of the exact time propagator. This issue is pertinent as the Floquet operator may have no normalizable eigenvectors if its spectrum is continuous. The question can be ideally answered by calculating the exact time propagation for an initial wave packet, $\Psi(t_0)$, corre-

sponding to a single truncated Floquet eigenvector, or in practice by giving error bounds for $\|\Psi(pT+t) - e^{-i\tilde{\varepsilon}pT}\Psi(t_0)\|$, where $\Psi(pT)$ is the exact wave function after p periods (T) of the perturbation and $\tilde{\varepsilon}$ is an approximate Floquet eigenvalue.

Localization phenomena in quantum dynamics has a long history. In the late 1970s the discovery[7] of unusual spectra for models in condensed matter physics prompted a tremendous interest in the investigation of transport phenomena in these systems. Also, during the 1980s and 1990s a huge number of papers in the field of quantum chaos analyzed the spectra of Floquet operators for a few paradigmatic driven systems trying to prove the conjecture that a diffusive quantum evolution similar to classical chaos could be possible if a singular continuous spectrum was present.[8] Nowadays, papers continue to be regularly published in these subjects,[9] but as far as we know no definitive answer has been given to the questions of when the Floquet operator of a driven system has exotic spectra (singular continuous, dense pure point, or Cantor) and how exotic spectra affect the quantum dynamics. These questions have interested mathematicians somehow independently of the mentioned progress in physics and probably earlier, and they have dedicated numerous efforts to the study of the spectra of Floquet operators resulting in several theorems that can be applied to current problems in physics. The ultimate goal of these studies is the analysis of the time evolution of quantum systems perturbed by periodic external fields in the limit $t \to \infty$.[10]

One of the systems that has been extensively studied during the last three decades is the planar rotor perturbed by a train of δ kicks.[11–13] Depending on the ratio between the moment of inertia of the rotor and the repetition frequency of the kicks two different regimes exist. A nonresonant regime corresponding to an irrational ratio for which the wave func-

a)Electronic mail: ortigoso@iem.cfmac.csic.es.

tion stays localized near the initial angular momentum states, and a resonant regime, that corresponds to a rational relation between both natural frequencies, for which the spectrum of the Floquet operator is continuous and wave functions do not stay localized. These two regimes can be understood with the use of a mapping between the kicked rotor and the Anderson model of solid state systems.[14] Quantum interference localizes wave functions similarly to the Anderson localization that takes place for the states of the one-dimensional tight binding model with a random potential. When the external perturbation consists of smooth pulses with a certain width instead of δ kicks, wave functions, in the resonant case, occupy a limited strip of angular momentum values.[15] For larger values of the coupling, numerical calculations indicate that the eigenstates remain localized in the nonresonant case.[16] Fishman *et al.*[15] showed that these localization phenomena also occur for diatomic molecules driven by a periodic train of smooth microwave pulses. In the strong coupling limit the driven diatomic molecule exhibits two kind of states, strongly localized and "plateau" states, that are somehow extended in angular momentum space. The limited extension of these states is the cause why molecules do not gain too much energy after each microwave pulse, and contrarily to the classical result no diffusion in energy takes place in the quantum regime.

The laser driven molecule is closely related to the microwave driven molecule, but the coupling mechanism is different. Molecules must have a permanent dipole to interact with the microwaves, while molecules with polarizability anisotropy are affected by a strong laser thanks to the induced dipole that the electromagnetic field creates in the molecule. Induced dipoles are proportional to molecular polarizabilities and they are smaller than permanent dipoles. However, laser intensities are orders of magnitude higher than microwave intensities, and the effective perturbations are much stronger. Another difference comes from the selection rules, $\Delta J = \pm 1$ for microwave transitions, but $\Delta J = 0, \pm 2$ for dipole-induced transitions, where J is the value of the rotational angular momentum. Thus, odd and even energy levels are not coupled by the laser. An interesting line of research would be to investigate the properties, in the present context, of rotational wave packets generated by excitation with frequencies near electronic resonances[17] or near rotational transitions.[18]

Although evidence from the work of Fishman and co-workers indicate that the Floquet spectrum of the microwave driven molecule is pure point, the existence of a singular continuous component has not been ruled out. Since the publication of Ref. 5 we wondered how the existence of a singular component in the Floquet spectra could affect the conservation of molecular alignment during a long train of laser pulses. This was the main motivation of the present work. Several mathematical theorems have been published in the last years that are directly applicable to this problem. These abstract studies normally are not interesting to chemical physicists, but we think that the level of experimental and theoretical sophistication that is being achieved in the study of time-dependent phenomena requires us to use all the available tools. Thus, we apply to our system a theorem by Howland[19] to discard the existence of absolutely continuous

spectra for any perturbation strength, and another theorem due to Duclos *et al.*[20] to prove that for very small laser intensities the spectrum is pure point. For the regime in which interesting physics takes place we show how to calculate error bounds for the time evolution of exact wave functions.

In Sec. II a brief review of Floquet theory emphasizing the expressions used in our calculations is presented. In Sec. III spatial alignment of molecules via the interaction of molecular polarizability with a train of laser pulses is discussed. In Sec. IV we comment on some basic concepts related to the spectra of self-adjoint operators, with an emphasis in the implications for rotational dynamics, and some fairly sophisticated mathematical machinery is applied to unravel the nature of the spectrum of the Floquet operator. In Sec. V expressions are presented to calculate error bounds for the time evolution of rotational wave packets. In Sec. VI results are given. Section VII summarizes and gives the conclusions of this work. Finally, the two theorems used in Sec. IV are presented in Appendix.

II. CYCLIC STATES FOR TIME-DEPENDENT SYSTEMS

In 1965 Shirley[21] showed how to transform a two-level system interacting with a time-dependent periodic electromagnetic field into a time-independent one represented by an infinite matrix. A few years later, Sambe introduced,[22] in an important paper, a formalism especially suited for the analysis of time-periodic systems. In Sambe's approach time is treated as a new spatial coordinate, t', and a Hamiltonian-like operator, the Floquet Hamiltonian K, is defined. It acts in an extended Hilbert space $\mathcal{K}$ which is formed by the tensorial product of the Hilbert space $\mathcal{H}$ corresponding to the spatial part of the Hamiltonian, and the space formed by all possible periodic functions (with period T) of the time coordinate with finite norm, $L^2([0,T], dt')$. Sambe showed that eigenstates of the Floquet Hamiltonian (called steady states, quasiperiodic states, or quasienergy states) in the extended Hilbert space are conceptually equivalent to the stationary states of conservative quantum systems. The Floquet approach for time-dependent Hamiltonians found a rigorous mathematical foundation in the work of Howland[23] and Yajima.[24] The Floquet Hamiltonian and the Floquet operator are unitarily equivalent, and thus, in this article, we will use for the eigenstates of both the term *Floquet eigenvectors*.

The elements of the extended Hilbert space $\mathcal{K}$ are T-periodic functions, χ, for which $\int_{-T/2}^{T/2} |\chi(\mathbf{q},t')|^2 d\mathbf{q} dt' < \infty$, where $\mathbf{q}$ represents the spatial coordinates. Thus, $\mathcal{K}$ is equipped with the inner product,[22]

$$\langle\langle \chi, \chi' \rangle\rangle := \frac{1}{T}\int_{-T/2}^{T/2}\int \chi^*(\mathbf{q},t')\chi'(\mathbf{q},t')d\mathbf{q}dt'. \quad (1)$$

A suitable complete basis set in $\mathcal{K}$ is given by functions $\langle\mathbf{q}|\phi\rangle\langle t'|n\rangle$, where the ϕ's form a basis set in $\mathcal{H}$ and $\langle t'|n\rangle$ are Fourier functions that span $L^2([0,t'], dt')$.

Wave functions in $\mathcal{K}$ obey a Schrödinger-like equation,[25]

$$\iota\hbar\frac{\partial}{\partial t}\chi(\mathbf{q},t';t) = K(\mathbf{q},t')\chi(\mathbf{q},t';t), \qquad (2)$$

where the progress parameter t is the physical time and the Floquet Hamiltonian K formally defined as $K:=-\iota\,\partial/\partial t' + H(t')$ depends on the variable t'. The solution of Eq. (2) for an initial wave function $\chi(\mathbf{q},t';t_0)$ can be written as

$$\chi(\mathbf{q},t';t) = \exp[(-\iota/\hbar)K(t')(t-t_0)]\chi(\mathbf{q},t';t_0). \qquad (3)$$

In the (t,t') method of Peskin and Moiseyev[26] the solution of the time-dependent Schrödinger equation in the usual Hilbert space is related to the solution in the extended Hilbert space $\chi(\mathbf{q},t';t)$ by

$$\Psi(\mathbf{q};t) = \chi(\mathbf{q},t';t)|_{t'=t}, \qquad (4)$$

where the cut $t'=t$ projects the wave function down to the standard Hilbert space. Notice that many different χ's can be projected from $\mathcal{K}$ giving the same function Ψ that obeys the time-dependent Schrödinger equation in $\mathcal{H}$, whereas elevation from a wave function in $\mathcal{H}$ to $\mathcal{K}$ is a one to many map.[25] This means that many different initial conditions can be taken in Eq. (2) for a given wave function $\Psi(t_0) \in \mathcal{H}$. A common choice is to take a function independent of t', $\chi(\mathbf{q},t';t_0)=\Psi(\mathbf{q};t_0)$, where Ψ is an eigenstate of the field-free system (or a linear combination of eigenstates). This choice is appropriate for an external field $V(t)$ for which $V(t=0)=V(t=T)=0$, and it implies an arbitrary phase between the initial wave function and the field.[27]

In general, assuming that K can be diagonalized (but see Sec. IV) the time-evolved wave function in $\mathcal{K}$ can be written, using bracket notation, as

$$|\chi\rangle\rangle = \sum_\lambda \exp[(-\iota/\hbar)\varepsilon_\lambda(t-t_0)]\,|\lambda\rangle\rangle\langle\langle\lambda|\Psi,n=0\rangle\rangle, \qquad (5)$$

where the $|\lambda\rangle\rangle$'s and the ε_λ's are the Floquet eigenpairs. Note that the cuts $|\phi(t_0)\rangle = |\lambda\rangle\rangle|_{t'=t_0}$ are eigenfunctions of the Floquet operator, $U(t_0+T,t_0)$, in the spatial Hilbert space and therefore they are cyclic wave packets. On the other hand, it can be shown, by using the periodicity of the Floquet eigenvectors, that the sum in Eq. (5) can be restricted to the first Brillouin zone, $(\varepsilon_\alpha \in [-\pi/T, \pi/T))$.[28] Thus, the solution of the time-dependent Schrödinger equation is

$$|\Psi(t)\rangle = \sum_{\alpha \in \text{FBZ}} \exp[(-\iota/\hbar)\varepsilon_\alpha(t-t_0)]\langle\phi_\alpha(t_0)|\Psi(t_0)\rangle$$
$$\times\,|\lambda_\alpha\rangle\rangle|_{t'=t}. \qquad (6)$$

III. ROTATIONAL CYCLIC STATES AND ALIGNED WAVE PACKETS

Quantum wave packets spread when they evolve in time. However, this spreading can be overcome in some cases by using external fields. Nonspreading wave packets are a subset of the steady states or eigenstates of the Floquet operator discussed in Sec. II. Buchleitner et al.[29] have shown how to build nonspreading wave packets for a Rydberg electron driven by a microwave field. According to them, from a quantum mechanical viewpoint, the construction of nonspreading wave packets for a particular system requires to find Floquet states that remain strongly localized during a period. Rotating molecules are well suited to create non-spreading wave packets.[5] It is well known that interaction of molecular polarizability with a nonresonant laser gives rise to pendular states[30] (rotational wave packets that librate around the field direction). The rotational wave function for a pendular state is concentrated about $\theta=0$, and π (where θ is the polar angle between the field direction and the internuclear axis) with small dispersion. Depending on the duration of the laser pulse the dynamics can be nonadiabatic and the molecule is placed, after the end of the pulse, in a field-free pendular state that subsequently dephases in such a way that the alignment is quickly lost.[31] Since only a few angular momentum eigenstates compose each pendular state, revivals in alignment take place, which can be experimentally exploited since alignment is periodically recovered. Therefore, if the Floquet eigenstates coincide with pendular states (or at least they are similar to them, depending on the robustness of the procedure), they will not loose their alignment during the whole duration of the pulse train.[6] But, there is no a priori guarantee that a particular time-dependent system will have localized Floquet eigenstates. Moreover, when the size of the spatial Hilbert space $N\to\infty$ Floquet eigenstates whatsoever may not exist as will be explained in Sec. IV.

The Floquet Hamiltonian $K(t')$ in dimensionless form (which suggests to use $\hbar/B$ as a reduced unit of time and $B/\hbar$ as a reduced unit of frequency, where B is the inverse of the moment of inertia), specialized for a diatomic or, more generally, for a linear polyatomic molecule, in the presence of a pulse train composed of linearly polarized nonresonant laser pulses, is

$$K(t') = -\iota\frac{\hbar}{B}\frac{\partial}{\partial t'} + \mathbf{J}^2 - (\Delta\omega\cos^2\theta + \omega_\perp)g(t'), \qquad (7)$$

where $\mathbf{J}$ is the angular momentum operator, and $\Delta\omega = \omega_\parallel - \omega_\perp$, with $\omega_{\parallel,\perp}=\alpha_{\parallel,\perp}\epsilon_L^2/4B$. The constants $\alpha_\parallel$ and $\alpha_\perp$ are the parallel and perpendicular components of molecular polarizability and ϵ_L is the peak strength of the laser field. The conversion factor for $\Delta\omega$ if the laser intensity I is expressed in W/cm^2 is[32]

$$\Delta\omega \approx 5 \times 10^{12}\Delta\alpha \ (cm^3)I \ (W/cm^2)/B \ (cm^{-1}), \qquad (8)$$

and the temporal profile can be written as $g(t')=\Sigma_{m=0}^\infty \times\exp(-(t'-mT)^2/\sigma^2)$, where σ is roughly the duration of each pulse and T defines the fundamental frequency, $\omega=2\pi/T$, of the perturbation.

Eigenfunctions of $K(t')$ can be expressed as linear combinations of the basis functions $\langle\theta,\xi|J,M\rangle\langle t'|n\rangle$, where $\langle\theta,\xi|J,M\rangle$ are eigenfunctions of $\mathbf{J}$ and its projection J_z along the laboratory-fixed axis defined by the polarization direction; and where the internal coordinates are the polar and azimuthal angles that give the relative orientation of the internuclear axis with respect to the laboratory-fixed axis system. The Fourier basis functions are $\langle t'|n\rangle = e^{2\pi\iota n t'/T}$. Thus,[33]

$$\langle\langle\theta,\xi,t'|\lambda\rangle\rangle = \sum_{J=0}^\infty \sum_{M=-J}^J \sum_{n=-\infty}^\infty \langle\langle\theta,\xi,t'|J,M,n\rangle\rangle\langle\langle J,M,n|\lambda\rangle\rangle.$$

$$(9)$$

When the initial wave function is a single cyclic state, $\phi(t_0)$, the solution, Eq. (6), of the time-dependent Schrödinger equation simplifies to

$$\Psi(\theta,\xi;t) = \exp[-\imath\varepsilon(t-t_0)]\phi(\theta,\xi;t), \qquad (10)$$

where $\phi(\theta,\xi;t) = \langle\langle\theta,\xi,t'|\lambda\rangle\rangle|_{t'=t}$.

When the light is linearly polarized the selection rule $\Delta M=0$ divides the matrix representation of K in independent M blocks. Thus, from now on we will consider only the block $M=0$ and we will write $|J\rangle$ for the rotational kets. Floquet eigenkets resulting from the diagonalization of a truncated matrix representation of K can then be written simply as

$$|\widetilde{\lambda}\rangle\rangle = \sum_{J=0}^{J_{max}} \sum_{n=-n_{max}}^{n_{max}} c_{Jn}|J\rangle|n\rangle, \qquad (11)$$

where the c_{Jn} are the numerical coefficients obtained from the diagonalization. In the same way, the initial state can be written as

$$|\widetilde{\phi}(t_0)\rangle = \sum_{J=0}^{J_{max}} d_J(t_0)|J\rangle, \qquad (12)$$

where

$$d_J(t) = \sum_{n=-n_{max}}^{n_{max}} c_{Jn}\exp(2\pi\imath nt/T). \qquad (13)$$

Finally, the approximate wave function at time t, Eq. (10), becomes

$$|\widetilde{\Psi}(t)\rangle = \exp[-\imath\widetilde{\varepsilon}(t-t_0)]\sum_{J=0}^{J_{max}} d_J(t)|J\rangle. \qquad (14)$$

Some of these wave packets are strongly aligned along the field direction provided the field has the appropriate strength and duration.[5] Alignment can be maintained for the whole duration of the pulse train if T has the appropriate value. Localized cyclic states resemble pendular states.[6] Thus, localization is more likely to happen for ultrashort pulses, where the shape of the laser is irrelevant, and the time propagator is well approximated by the sudden propagator, some of whose eigenstates are pendular states.[34] Nonetheless, cyclic states with strong alignment exist far from this limit. The upper panel of Fig. 1 shows the time dependence of the expectation value of $\cos^2\theta$, which is a measurement of alignment, for two different cyclic states. The middle and lower panels show the composition of these cyclic states at two different times, before the first pulse starts and at the maximum of the last pulse shown in the figure. The aligned state (in red) has, at initial time, a significant contribution ($>1\%$) of only six $|J\rangle$ states, with the largest contribution due to the state $|J=4\rangle$. At the time when the laser intensity reaches its maximum value only five rotational states contribute more than 1% and now the biggest contribution comes from $|J=2\rangle$. However, this state has a long tail formed by high rotational states whose contribution is small. At $t=-T/2$ the coefficients corresponding to the rotational basis functions $|J=20\rangle$, $|J=40\rangle$, $|J=60\rangle$, and $|J=80\rangle$ are -0.0230,
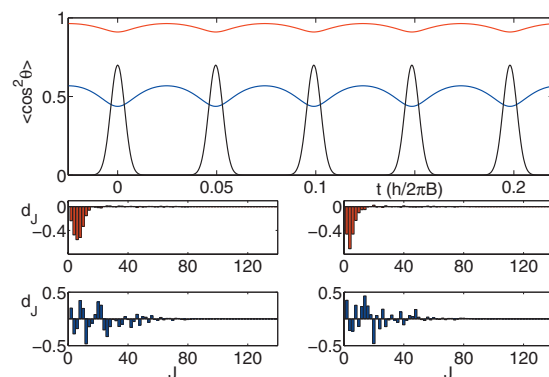

FIG. 1. Upper panel shows the time dependence of molecular alignment, given by $\langle\cos^2\theta\rangle$, during several laser pulses for two different initial states. The time envelope of the laser is the black line. The calculation corresponds to the parameters in Eq. (7) $\sigma=0.005$, $T=0.05$ in $(\hbar/B)$ units, and $\Delta\omega=2000$. The middle panel shows the composition of the wave function that gives maximum alignment (red), in the rotational basis set, at two times, before the launch of the laser field (left) and when the maximum of the last laser pulse takes place. The lower panel shows the same for the wave function for which the alignment is smaller (blue). A global phase factor has been eliminated for the wave functions at the time when the intensity reaches the maximum value.

0.0062, 0.0079, and -0.0010, respectively, and basis functions with $J>120$ have coefficients with absolute value smaller than 10^{-9}. The misaligned state, blue, in Fig. 1, is even more extended in J space. For example $d_{J=0}=0.2027$, $d_{J=40}=-0.1593$, $d_{J=60}=0.0274$, and $d_{J=100}=-0.0004$. However, for $J>124$ the coefficients are already smaller than 10^{-9} and for $J=182$ the coefficient is smaller than 10^{-14}. Figure 2 shows that the two Floquet states from which the cyclic states of Fig. 1 were calculated are fairly extended in the $|J\rangle|n\rangle$ basis set.

IV. EXISTENCE OF ROTATIONAL CYCLIC STATES WHEN $N\rightarrow\infty$

A. Some basic definitions regarding the spectra of self-adjoint operators

The pure point spectrum of a self-adjoint operator A is the set of all its eigenvalues, i.e., the z values for which $A\zeta$
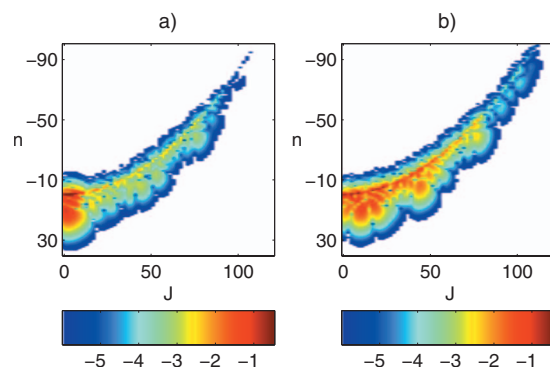

FIG. 2. Density plots of two eigenstates of K, Eq. (7), in the $|J\rangle|n\rangle$ basis set, for $\sigma=0.005$, $T=0.05$, $\Delta\omega=2000$, $J_{max}=260$, and $n_{max}=400$. The two cyclic states shown in Fig. 1 were calculated from these states. The eigenstate in (b) is the misaligned state and it occupies a larger number of basis functions than the aligned state in (a). In order to make visible the long tails the plots represent $\log|c_{Jn}|$, Eq. (11). Coefficients for which $|c_{Jn}|\leq 10^{-6}$ have been eliminated.

$=z\zeta$, where ζ is a normalizable function belonging to the Hilbert space of the system. Eigenvalues can be defined by using Weyl sequences.[35] A Weyl sequence for an operator A at z is a sequence of normalized vectors ζ_n belonging to the domain of A, for which $\lim_{n\to\infty}\|(A-zI)\zeta_n\|=0$. Then, z is an eigenvalue of A and $\zeta=\lim_{n\to\infty}\zeta_n$ an eigenvector. On the other hand, when the only solution of $A\zeta=z\zeta$ is $\zeta=0$, z may belong to the continuous spectrum and then it is a generalized eigenvalue only if there is a singular Weyl sequence[35] at z. A Weyl sequence is singular if ζ_n converges weakly to zero, i.e., $\forall \varphi \in \mathcal{H}$, $\lim_{n\to\infty}\langle\zeta_n|\varphi\rangle=\langle\zeta=0|\varphi\rangle$. Note that every z belonging to the continuous spectrum of A is a generalized eigenvalue.

The survival probability gives the probability of finding the system at time t in its initial state Ψ. It coincides with the square of the absolute value of the Fourier transform of the spectral measure (or local density of states) μ_Ψ for the vector Ψ,

$$|\langle\Psi(0)|\Psi(t)\rangle|^2 = \left|\int_{\sigma(A)} e^{-i\gamma t} d\mu_\Psi(\gamma)\right|^2. \tag{15}$$

Thus, the spectral measure, which loosely can be defined as the size of the spectrum, can be obtained from the survival probability. It increases monotonically from 0 to 1 as γ goes over the spectrum. The points where μ increases form the local spectrum or, technically, the support of μ. The spectrum σ is the union of the supports of μ for a set of Ψ's that form a basis in $\mathcal{H}$. The spectral measure is singular $(d\mu/d\gamma=0)$ when its support is a set of measure zero, otherwise it is continuous.[36] Thus, in general, the spectral measure can be decomposed into a singular component and a continuous component. However, in some cases the spectral measure has a singular continuous component, i.e., a continuous part of measure zero. This decomposition of the spectral measure establishes a decomposition of the Hilbert space of the system into three orthogonal subspaces $\mathcal{H}\equiv\mathcal{H}_{pp}\oplus\mathcal{H}_{ac}\oplus\mathcal{H}_{sc}$ (where pp stands for pure point, ac for absolutely continuous, and sc for singular continuous). On the other hand, the continuous subspace is defined as $\mathcal{H}_c\equiv\mathcal{H}_{ac}\oplus\mathcal{H}_{sc}$, and the singular subspace as $\mathcal{H}_s\equiv\mathcal{H}_{pp}\oplus\mathcal{H}_{sc}$. Thus, the spectrum can be written as $\sigma=\sigma_{pp}\cup\sigma_{ac}\cup\sigma_{sc}$. The spectrum also can be decomposed as $\sigma=\sigma_{disc}\cup\sigma_{ess}$, where the discrete spectrum σ_{disc} is the set of isolated eigenvalues of finite multiplicity and the essential spectrum σ_{ess} contains the rest of the spectrum. Note that pure point spectrum and discrete spectrum are not synonymous concepts although both are composed by the eigenvalues of the operator. If the pure point spectrum is dense the eigenvalues are not isolated (see below) and it belongs to the essential spectrum.

Pure point spectra and continuous spectra are common objects in atomic and molecular physics; the first are related to the bound energy levels of an atom or molecule and the second to scattering states. Singular continuous spectra were considered rather exotic objects in the past[37] and usually they are not mentioned in physic books. However, since the 1990s numerous operators with a singular continuous spectral component have been found, especially in condensed matter systems.[38]
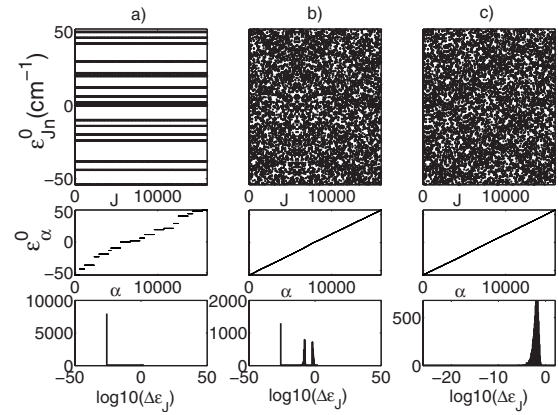

FIG. 3. In the upper row are shown the eigenvalues of K_0 in the first Brillouin zone (see text) as a function of J, calculated with $J_{max}=16\,000$, $n_{max}=\infty$. Column (a) is for a frequency resonant with the transition $J=10\leftarrow J=0=110(B/\hbar)$. Column (b) is for a nonresonant frequency, such that $\omega=110(q/p)(B/\hbar)$, where $p=11\,000$ and $q=11\,639$. Column (c) corresponds to $p=1.1\times10^8$, $q=116\,390\,209$. The middle row represents the same eigenvalues but the label of the x axis is an index that identifies eigenvalues by their quasienergy ordering. The lower row gives the level spacing distributions.

B. Perturbation of operators with dense spectrum

When the spectrum of the field-free Hamiltonian is discrete but unbounded ($\varepsilon_n\to\infty$ when $n\to\infty$) the spectrum of the corresponding zeroth-order Floquet Hamiltonian $K_0(t)$ $:=H_0-i\partial/\partial t$ is pure point and dense (see Ref. 39 for a proof), i.e., in each spectral interval there is at least one eigenvalue of K_0. Obviously this is the case for an ideal linear rotor perturbed by a train of nonresonant laser pulses, for which the eigenvalues of K_0 are $\varepsilon_{J,n}^0=J(J+1)+2\pi n/T$, where the angular momentum value (in $B/\hbar$ units) $J=0,1,\ldots,\infty$ and $n=-\infty,\ldots,\infty$. The $\varepsilon_{J,n}^0$'s form a dense set unless there is a rational relationship between the repetition frequency of the laser field, $2\pi/T$, and the field-free rotational energy levels. In this case the function μ raises continuously over a finite number of points being flat in between and the quasienergies form bands separated by gaps. Figure 3 illustrates the behavior of the quasienergies within the first Brillouin zone that can be calculated as $\varepsilon_\alpha^0=\{[J(J+1)+T/2]\mathrm{mod}(2\pi/T)\}-T/2$. Columns (a), (b), and (c) correspond to different laser periods. Case (a) is for a frequency, $\omega=2\pi/T$, coincident with the $J=10\leftarrow J=0$ transition. Column (b) corresponds to $\Delta\varepsilon_{10\leftarrow0}^0/\omega=p/q$, where $p=11000$ and $q=11639$. Finally, column (c) corresponds to $p=1.1\times10^8$ and $q=116\,390\,209$. Plots in the upper row show the zeroth-order quasienergies ε_α^0 up to $J=16\,000$, in the first Brillouin zone. The effective number of $|n\rangle$ basis functions is given by $n_{max}=TJ_{max}(J_{max}+1)/2\pi$, which means that an infinite effective number of n's has been considered in the calculation because for the J's considered $\varepsilon_{J,n}^0$ with $|n|>n_{max}$ is outside the first Brillouin zone. The resonance case in (a) shows a structure of quasienergy bands separated by gaps, whereas in (b) and (c) the spectra fill almost densely the plane with no gaps. The middle row shows the same spectra ordered by quasienergy and finally the lower row shows the level spacing. For the resonant frequency there is a sharp peak in the level spacing distribution at zero, while
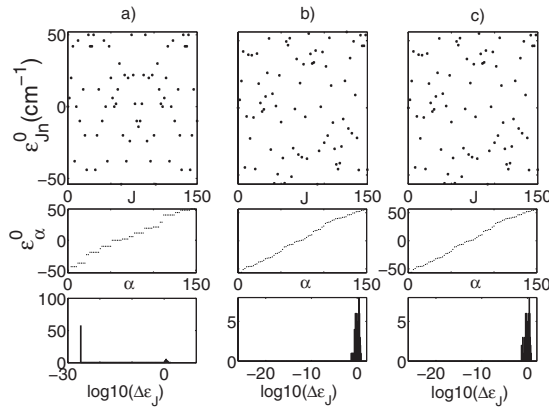
FIG. 4. Same as Fig. 3 but $J_{max}=150$ instead of 16 000.

for the nonresonant frequency with the smaller p,q the sharp peak at zero still exists but two additional bands arise due to the limited number of J's employed. In the nonresonant case with larger p,q [column (c)] the peak at zero is missing and there is a wide band around 10^{-3}. This effect is due to the limited number of $|J\rangle$ states included in the calculation. In the limit $J\rightarrow\infty$ both nonresonant cases would look equivalent. Thus, when the frequency of the external perturbation is not exactly resonant with a proper frequency of the system the Floquet spectrum is dense with no gaps. However, when J_{max} is finite but large there are differences in the level spacings depending on the irrationality of the frequency. Thus, the larger the two integers p,q are, the less dense the spectrum is (for finite J). Figure 4 shows similar plots for $J_{max}=150$. In this case, the middle and the right column look very similar as the high order resonances responsible for the differences found in Fig. 3 are absent.

When the zeroth-order Floquet Hamiltonian K_0 has a dense spectrum the nature of the spectrum of the perturbed operator K cannot be studied with the traditional Rayleigh–Schrödinger perturbative techniques because the denominators $\varepsilon_\alpha^0-\varepsilon_\beta^0$ that arise in the perturbation series can be very small spoiling their convergence. Quantum KAM (Kolmogorov, Arnold, Moser) methods have been used with success to show that, for some systems, K has a pure point spectrum for small values of the perturbation after a small set of resonant frequencies is excluded.[40] Soon after Shirley's paper[21] was published, Young *et al.*[41] conjectured that, in general, these systems do not have true quasiperiodic states.

C. Consequences of the existence of a singular continuous component in the spectrum of the Floquet Hamiltonian

The dynamics of periodic time-dependent quantum systems are related to the spectra of their Floquet Hamiltonians. Quantum states of bounded quantum systems evolve quasiperiodically and reassemble infinitely often.[42] Contrarily, for unbounded systems with absolutely continuous spectrum quantum states decay, and their survival probability goes to zero in the limit $t\rightarrow\infty$. If the spectrum is singular continuous the survival probability goes to zero on the average but it may or may not tend to zero in the limit $t\rightarrow\infty$,[43] i.e., some states will be decaying but others will not decay. Thus, the

singular continuous spectra can behave as point spectra or as absolutely continuous spectra. Fishman and coworkers[44] have provided exactly solvable models that illustrate the main characteristics of systems with a singular continuous component. These studies show that singular continuous wave functions for a rotor have peaks that increasingly spread apart when $J\rightarrow\infty$. In general, wave functions of a system whose Floquet Hamiltonian has a singular continuous spectrum first spread and then they concentrate again.

When the Floquet Hamiltonian has a purely continuous spectrum, truly cyclic states do not exist because $U(T+t_0,t_0)\phi=e^{\iota\delta}\phi$ does not hold for any $\phi\in\mathcal{H}$. Yet, it is possible to find approximate cyclic states by projecting into $\mathcal{H}$ pseudoeigenvectors $\widetilde{\lambda}\in\mathcal{K}$, for which $\|(K-\widetilde{\varepsilon})\widetilde{\lambda}\|<\epsilon$. These states remain quasicyclic during a number of periods that can be very large depending on the size of ϵ, but pseudoeigenvectors obtained from finite-basis representations of K cannot be cyclic in the limit $t\rightarrow\infty$ as we show below. Note the difference with the case in which the Floquet Hamiltonian has pure point spectrum for which eigenstates can be obtained within an arbitrarily small error by using finite matrix representations.[45]

If $U(T+t_0,t_0)$ only has continuous spectrum any vector Ψ belonging to $\mathcal{H}$ obeys[46]

$$\frac{1}{\tau}\int_0^\tau \langle U(t,t_0)\Psi|\widetilde{U}(t,t_0)\Psi\rangle dt = 0 \qquad (16)$$

for large enough τ, where $\widetilde{U}$ stands for an approximate propagator built from the eigenstates of a truncated matrix representation of U, $\widetilde{U}(t,t_0)=\Sigma_\alpha|\widetilde{\phi}_\alpha(t)\rangle e^{-\iota\widetilde{\varepsilon}_\alpha(t-t_0)}\langle\widetilde{\phi}_\alpha(t_0)|$. $P_{\widetilde{\phi}}=|\widetilde{\phi}(t)\rangle\langle\widetilde{\phi}(t_0)|$ is a finite-dimension projector in $\mathcal{H}$. If we take as initial wave function one of the cyclic states, $|\Psi(t_0)\rangle=|\widetilde{\phi}(t_0)\rangle$, we have, for all t, that $\|(I-P_{\widetilde{\phi}})\widetilde{U}(t,t_0)\Psi\|=0$, and

$$\frac{1}{\tau}\int_0^\tau \langle(P_{\widetilde{\phi}}+I-P_{\widetilde{\phi}})U(t,t_0)\Psi|\widetilde{U}(t,t_0)\Psi\rangle dt$$

$$=\frac{1}{\tau}\int_0^\tau \langle P_{\widetilde{\phi}}U(t,t_0)\Psi|\widetilde{U}(t,t_0)\Psi\rangle dt$$

$$+\frac{1}{\tau}\int_0^\tau \langle(I-P_{\widetilde{\phi}})U(t,t_0)\Psi|\widetilde{U}(t,t_0)\Psi\rangle dt$$

$$\leq \|\widetilde{U}(t,t_0)\Psi\|\frac{1}{\tau}\int_0^\tau \|P_{\widetilde{\phi}}U(t,t_0)\Psi\|dt + \|U(t,t_0)\Psi\|$$

$$\times\frac{1}{\tau}\int_0^\tau \|(I-P_{\widetilde{\phi}})\widetilde{U}(t,t_0)\Psi\|dt. \qquad (17)$$

The second integral in the previous expression is zero as the integrand is zero at all times. The first one tends to zero when $\tau\rightarrow\infty$ by RAGE (Ruelle, Amrein, Georgescu, and Enss) theorem[35] for periodic systems,[45] which establishes that wave functions belonging to the continuous subspace $\mathcal{H}_c$, defined in Sec. IV A, escape in average any subspace of $\mathcal{H}$ of finite dimension.

Singular continuous spectra have a multifractal structure, which makes them very fragile objects, which, no doubt, will be strongly affected by unavoidable numerical errors. In fact, Carey and Pincus[47] showed that a self-adjoint operator with purely singular continuous spectrum differs from a pure point operator by a trace-class operator (an operator with trace, $\Sigma_n \langle \varphi_n | A | \varphi_n \rangle < \infty$, where the φ's are the members of any complete basis of the Hilbert space) with arbitrarily small norm. Tiny perturbations that likely are present in any real experiment can destroy the singular continuous spectra. Thus, the existence of a singular continuous spectrum is probably undetectable in experiments due to the different sources of spectral broadening (finite temperature, random imperfections of the experimental setup, etc.).[36]

Summarizing, when the spectrum of $U(t_0+T,t_0)$ is purely continuous its approximate eigenfunctions $\tilde{\phi}$, obtained from the eigenfunctions $\tilde{\lambda}$ of a truncated Floquet Hamiltonian, cease to be cyclic after a number of periods. We will show in Sec. V that the smaller $\|(K-\tilde{\varepsilon})\tilde{\lambda}\|$ is the longer $\tilde{\phi}$ will remain cyclic under the exact time evolution.

D. Rigorous results on the nature of the spectrum of the Floquet Hamiltonian for a molecule in a laser pulse train

In this subsection we discuss the results of applying two abstract theorems to the study of the nature of the spectrum of K for the case of a linear molecule interacting with a train of linearly polarized nonresonant laser pulses. The theorems and their application to our system are given in Appendix. Hone et al.[4] have given solid arguments about the nature of the Floquet spectrum when the size of the spatial Hilbert space $N \to \infty$. The essence of the arguments, given in Propositions I and II of the cited paper, is that in any given β interval [where β gives the strength of the time-dependent perturbation, i.e., $K(t)=K_0(t)+\beta V(t)$], there exists a dense set of β values (with measure zero) for which Floquet states do not converge as a function of N (Proposition II); and that as N grows there is an increasing measure of β where a finite-basis calculation gives Floquet states within an arbitrarily small error (Proposition I). These results combined with Theorem 1 in Appendix imply that for any β interval there is a dense set of β values for which the spectrum of the Floquet Hamiltonian is singular continuous but a set with the measure of the full interval for which the spectrum is pure point.

In Appendix it is shown that Theorem 1 applies to the Floquet Hamiltonian equation (7), and thus it has no absolutely continuous spectrum for any finite $\Delta\omega$. The nonexistence of an absolutely continuous part in the spectrum of an operator is a weaker result than the pure point character of the spectrum, since it does not rule out the existence of a singular continuous spectrum. On the other hand, it was shown in Ref. 48 that the spectrum is generically dense pure point in a probabilistic sense provided the gap between consecutive energy levels of the field-free system $\varepsilon_n-\varepsilon_{n-1} > Cn^\kappa$, for $\kappa > 2$, which unfortunately does not cover rotational dynamics.[20]

For elliptical polarization of the external field, extensions of the theorem are needed since in this case the pertur-

bation can mix rotational states with different magnetic quantum numbers. In other words, since the magnetic degeneracy of the field-free rotational levels must be taken into account the condition on the multiplicity of the eigenvalues used by Howland does not hold. However, this condition is a technical one and can be removed provided $V(t)$ is smooth enough.[49] Thus, Nenciu showed[50] that if the spectrum of the zeroth-order Floquet operator K_0 ($V(t)=0$) obeys the increasing gap condition for some $C>0$, $\kappa>0$, and the degeneracy M_J of its eigenvalues is such that $M_J \leq AJ^\eta$ with $A < \infty$, $0 \leq \eta < \infty$, the external perturbation $V(t)$ needs to be C^r with $r \geq [(1+\eta)/\kappa]+1$ for the spectrum of K to have no absolutely continuous part. Thus, $\varepsilon_J \approx J^2, M_J \approx J$ when $J \to \infty$, which implies $\kappa=1$, $\eta=1$. Therefore, for a perturbation $V(t) \in C^3$ the Floquet Hamiltonian of the three-dimensional rotor has no absolutely continuous spectrum.

Recently Duclos et al. have given a rigorous proof, using a quantum KAM formalism,[40] of the pure point character of the spectrum for regular enough $V(t)$, where this regularity is related to the matrix elements of V in the extended Hilbert space.[20] In the KAM method a sequence of operators K_n is constructed that converges to a diagonal operator which has a pure point spectrum. This operator is unitarily equivalent to the Floquet Hamiltonian, proving therefore that it has pure point spectrum. The application of Theorem 2 in Appendix to our system shows the existence of an interval Ω_∞, such that for $\Delta\omega \in \Omega_\infty$ the spectrum of the Floquet operator is pure point except for a set corresponding to high-order resonant frequencies. As shown in Appendix the values of $\Delta\omega$ for which the existence of pure point spectrum has been proven are too small and no interesting physics will take place for perturbations of that size. However, it gives a rigorous proof, albeit for a very reduced range of laser intensities, of Propositions I and II of Hone et al.[4]

V. ERROR BOUNDS FOR FINITE-BASIS CALCULATIONS OF FLOQUET STATES

Our goal is to determine up to which extent approximate cyclic states obtained from eigenvectors of a truncated Floquet Hamiltonian remain cyclic after several periods of the time-dependent perturbation. Consider an initial wave function $\Psi(t_0)$ belonging to $\mathcal{H}$. Error bounds for $\|U(t_f,t_0)\Psi(t_0) - \tilde{U}(t_f,t_0)\Psi(t_0)\|$, where $\tilde{U}$ is an approximate propagator and U is the exact propagator, can be obtained from the following inequality due to Young et al.:[51]

$$\|\Psi(t_f) - \tilde{\Psi}(t_f)\| - \|\Psi(t_0) - \tilde{\Psi}(t_0)\| \leq B^{(1)}(t_0,t_f), \qquad (18)$$

where

$$B^{(1)}(t_0,t_f) = \int_{t_0}^{t_f} dt \left\| \left(H(t) - \iota \frac{\partial}{\partial t}\right)\tilde{\Psi}(t) \right\|. \qquad (19)$$

By taking $\Psi(t_0)=\tilde{\Psi}(t_0)$, Eq. (18) becomes

$$\|\Psi(t_f) - \tilde{\Psi}(t_f)\| \leq B^{(1)}(t_0,t_f), \qquad (20)$$

which gives an error bound for the difference between the approximate time evolution of any wave function and the exact evolution. Several expressions giving error bounds for

time-dependent calculations have been published. The review by Pfeifer and Frölich[52] gives a fairly complete account of previous results. Another interesting discussion on error bounds for finite-basis expansions in time-dependent calculations is given by Uhlmann *et al.*[53]

In the case studied by Young *et al.* the approximate wave function is given by the adiabatic approximation, but, in general, any approximate wave function can be substituted in $\widetilde{\Psi}(t)$. The norm in $B^{(1)}$ involves the integral of a square root of several summands, which can be eliminated by applying the Schwarz inequality $\int_{t_0}^{t_f} f(t)dt \leq \sqrt{(t_f - t_0)\int_{t_0}^{t_f} f(t)^2 dt}$, giving

$$\|\Psi(t_f) - \widetilde{\Psi}(t_f)\| \leq B^{(2)}(t_0, t_f), \tag{21}$$

where

$$B^{(2)}(t_0, t_f) = \sqrt{(t_f - t_0)\int_{t_0}^{t_f} dt \left\| \left(H(t) - \iota\frac{\partial}{\partial t}\right)\widetilde{\Psi}(t) \right\|^2}. \tag{22}$$

By substituting the expression for $\Psi(t)$, Eq. (6), in the previous expression, and taking $t_0 = -T/2$ and $t_f = (p-1)T + T/2$, we get

$$B^{(2)}(pT) = \sqrt{pT\int_{-T/2}^{(p-1/2)T} dt \left\| \sum_\alpha \exp[-\iota\widetilde{\varepsilon}_\alpha pT]\left(H(t) - \iota\frac{\partial}{\partial t} - \widetilde{\varepsilon}_\alpha\right)|\widetilde{\phi}_\alpha(t)\rangle\langle\widetilde{\phi}_\alpha(-T/2)|\widetilde{\Psi}(-T/2)\rangle \right\|^2}. \tag{23}$$

By choosing $\widetilde{\Psi}(-T/2) = \widetilde{\phi}(-T/2)$, where $\widetilde{\phi}$ is one of the cyclic states of the approximate propagator we get that after p periods $\widetilde{\Psi}(t_0 + pT) = e^{-\iota\widetilde{\varepsilon}pT}\widetilde{\Psi}(-T/2)$. Also, with this choice, due to the orthogonality of the cyclic states, the summation in Eq. (23) reduces to a single term,

$$\|\Psi((p-1/2)T) - e^{-\iota\widetilde{\varepsilon}pT}\Psi(-T/2)\|$$
$$\leq \sqrt{pT\int_{-T/2}^{(p-1/2)T} dt \left\| \left(H(t) - \iota\frac{\partial}{\partial t} - \widetilde{\varepsilon}\right)\widetilde{\phi}(t) \right\|^2}. \tag{24}$$

Taking into account that $\int_{-T/2}^{(p-1/2)T} = p\int_{-T/2}^{T/2}$ due to the periodicity of $\widetilde{\Psi}$, and recalling the definition of norm in the extended Hilbert space [Eq. (1) for $\chi = \chi'$], it is easy to check that the previous expression is equivalent to

$$\|\Psi((p-1/2)T) - e^{-\iota\widetilde{\varepsilon}pT}\Psi(-T/2)\| \leq pT\|(K-\widetilde{\varepsilon})\widetilde{\lambda}\|_\mathcal{K}. \tag{25}$$

This simple but remarkable result gives a bound on how well eigenstates of an approximate Floquet operator are cyclic after p periods of the perturbation. A convenient simplification from the numerical point of view can be done by realizing that

$$\|(K-\widetilde{\varepsilon})\widetilde{\lambda}\|_\mathcal{K} = \|QK\widetilde{\lambda}\|_\mathcal{K}, \tag{26}$$

where Q projects to the subspace complementary to that spanned by the finite basis employed to form the matrix representation of the Floquet Hamiltonian.

The calculation of the error bound requires to know the effect of the Q-projected exact Floquet Hamiltonian over the approximate Floquet eigenket $|\widetilde{\lambda}\rangle\rangle$, which for the case of a rotor in a periodic laser field can be done analytically. Thus, using Eq. (11) for $|\widetilde{\lambda}\rangle\rangle$, we get that the effect of the coupling term is

$$-\Delta\omega\cos^2\theta e^{-t'^2/\sigma^2}|\widetilde{\lambda}\rangle\rangle$$
$$= -\Delta\omega\Bigg\{ \left[\sum_{J=0}^{J_\text{max}}\sum_{n'=-n_\text{max}}^{n_\text{max}}(c_{Jn'}\langle J|\cos^2\theta|J\rangle + c_{J-2,n'} \right.$$
$$\times\langle J|\cos^2\theta|J-2\rangle + c_{J+2,n'}\langle J|\cos^2\theta|J+2\rangle)$$
$$\times\sum_{n=-\infty}^{\infty}\langle n|e^{-t'^2/\sigma^2}|n'\rangle\,|J,n\rangle\rangle \Bigg]$$
$$+ \sum_{n'=-n_\text{max}}^{n_\text{max}}c_{J_\text{max},n'}\langle J_\text{max}+2|\cos^2\theta|J_\text{max}\rangle$$
$$\left. \times\sum_{n=-\infty}^{\infty}\langle n|e^{-t'^2/\sigma^2}|n'\rangle\,|J_\text{max}+2,n\rangle\rangle \right\}, \tag{27}$$

where the matrix elements of $\cos^2\theta$ are given by Eqs. (A1)–(A4), and the matrix elements of $e^{-t'^2/\sigma^2}$ by Eq. (A15). Recall also that $c_{Jn'} = 0$ for $J > J_\text{max}, |n'| > n_\text{max}$. The effect of Q over the previous expression is simply to cut the first summation in n in such a way that this index runs from $-\infty$ to $-n_\text{max}-1$ and from $n_\text{max}+1$ to ∞. Thus, taking into account that

$$Q\left(\mathbf{J}^2 - \iota\frac{\partial}{\partial t'}\right)|\widetilde{\lambda}\rangle\rangle = 0, \tag{28}$$

we finally obtain for the error bound

$$B^{(2)}(pT) = pT\Delta\omega \left\{ \left[\sum_{J=0}^{J_{\max}} \sum_{|n|>n_{\max}} \left[\sum_{n'=-n_{\max}}^{n_{\max}} (c_{Jn'}\langle J|\cos^2\theta|J\rangle \right. \right. \right.$$

$$+ c_{J-2,n'}\langle J|\cos^2\theta|J-2\rangle + c_{J+2,n'}\langle J|\cos^2\theta|J+2\rangle)$$

$$\left. \times \langle n|e^{-t'^2/\sigma^2}|n'\rangle \right]^2 \right]^2 + \sum_{n=-\infty}^{\infty} \left[\sum_{n'=-n_{\max}}^{n_{\max}} c_{J_{\max},n'} \right.$$

$$\left. \left. \times \langle J_{\max}+2|\cos^2\theta|J_{\max}\rangle\langle n|e^{-t'^2/\sigma^2}|n'\rangle \right]^2 \right]^{1/2} \right\}. \quad (29)$$

In practice, we truncate in our calculations the infinite sums in n to the value for which $\langle n|e^{-t'^2/\sigma^2}|n'\rangle < 10^{-18}$ for each n' in the basis set. Equation (29) indicates that there are two somehow limiting cases in the calculation of the error bound. If $n_{\max}$ is large, and $J_{\max}$ is small the error comes basically from the terms with $|J_{\max}+2,n\rangle\rangle$ for $n \le n_{\max}$ in Eq. (27). In the inverse case the terms that contribute are those with $J \le J_{\max}$ and $n > n_{\max}$.

VI. RESULTS

In this section we present calculations of error bounds. The equality found between the error bound, Eq. (24), and the norm, Eq. (26), allows us to speak indistinctly of the error bound for the evolved wave function or of the error bound for the progenitor Floquet eigenstate. Cyclic eigenstates are obtained from truncated matrix representations of the Floquet Hamiltonian, Eq. (7). The matrix is diagonalized using the ARPACK package[54] that implements an Arnoldi–Lanczos algorithm on an inverted and shifted K matrix, $(I/(K-\varepsilon_0 I)]$. The algorithm first finds eigenpairs near ε_0. By choosing $\varepsilon_0=0$ eigenvalues in the first Brillouin zone are calculated. Eigenvectors for several sets of parameters of K were obtained to investigate different physical regimes.

First, we calculate eigenstates for the case of a train of ultrashort laser pulses ($\sigma=0.005\hbar/B=25$ fs for $B=1$ cm^{-1}) of moderate intensity ($\Delta\omega=250$) for which the spacing between pulses is also very short ($T=0.05\hbar/B$). In this case some cyclic states are strongly aligned pendular states. A small basis set ($J_{\max}=30$, $n_{\max}=50$) is enough to produce eigenstates for which the error bound, after one period of the perturbation, is of the order of $\sim10^{-11}$. This means that $\|\Psi(t_0+10^9 T)-\Psi(t_0)\| \le 5\times10^{-4}$, and the wave function is quasicyclic after 10^9 laser pulses or 10^{10} rotational periods.

The second case corresponds to wider pulses, $\sigma=0.2\hbar/B$, with a longer separation, $T=2\hbar/B$, and $\Delta\omega=250$. The matrix elements $\langle n|e^{-t^2/\sigma^2}|n'\rangle$, Eq. (A15), depend only on the ratio σ/T and therefore the coupling term of the Floquet Hamiltonian, Eq. (7), is the same as in the previous case. However, the zeroth-order level spacing between zeroth-order $|J,n\rangle\rangle$ levels with the same J is given by $2\pi/T$, which is smaller than in the previous case resulting in an increase in the interlevel coupling. As a consequence a greater number of $|n\rangle$ basis functions is needed. We show in Fig. 5 the quasienergies and error bounds of three cyclic states as functions of the size of the time basis set. A remarkable finding is that quasienergies converge much faster than their error
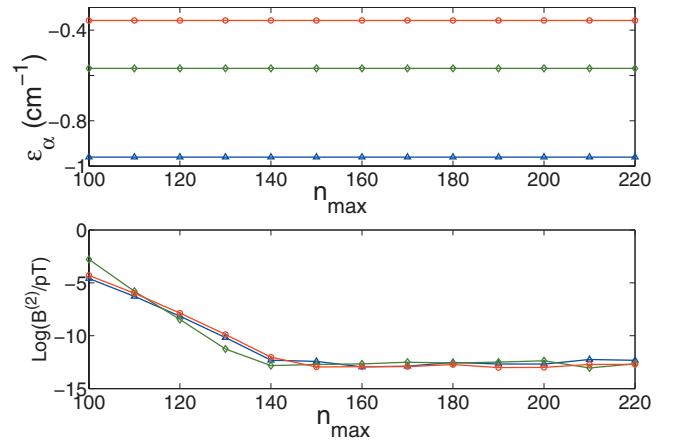

FIG. 5. Lower panel gives the logarithm of the error bounds for the three lowest quasienergy Floquet eigenstates of K, Eq. (7), for $\sigma=0.2$, $T=2$ (both in $\hbar/B$ units), $\Delta\omega=250$ and $J_{\max}=50$, as a function of the $n_{\max}$ value to which the matrix representation of K is truncated. The upper panel shows the corresponding quasienergies. The lines connect the different points according to quasienergy ordering and they are plotted only to guide the eye but have no other meaning. The same color is used in both panels to identify a given quasienergy and its error bound.

bounds. In fact, quasienergies almost do not vary when $n_{\max}$ increases, whereas the error bounds decrease steadily. This shows that convergence of eigenvalues of finite representations of Floquet Hamiltonians may not always be a useful criterion to determine the quality of a given calculation. We observe in Fig. 5 that, in order to obtain error bounds below 10^{-10}, we need $n_{\max}(\ge140)$, which is higher than for shorter pulses. Figure 6 shows the cyclic vectors at the beginning of the pulse for which error bounds were plotted in Fig. 5. The size of the $|n\rangle$ basis set needed to achieve small error bounds increases when σ/T decreases. This is illustrated in Fig. 7 that corresponds to laser pulses with $\sigma=0.02$ and $T=2$. A low intensity $\Delta\omega=50$ has been chosen in order to limit the number of $|J\rangle$ basis functions. Error bounds were calculated from matrices corresponding to $J_{\max}=40$ and different $n_{\max}$. These bounds are notoriously worse than those shown in Fig. 5. In fact, $n_{\max}=290$ is needed to achieve an error bound that varies between 10^{-5} and 10^{-7} depending on the state.

Finally, we show results for $\sigma=0.005$, $T=0.05$, and a

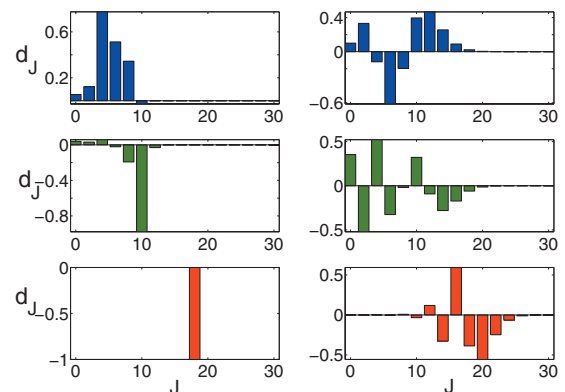FIG. 6. The three cyclic vectors that were used to plot Fig. 5 for $J_{\max}=50$ and $n_{\max}=140$. The left column gives the composition of the cyclic states at $t=-T/2$, and right column at $t=0$. A global phase factor has been eliminated for the wave functions at $t=0$. Colors are used to identify the cyclic states with their quasienergies and error bounds shown in Fig. 5.
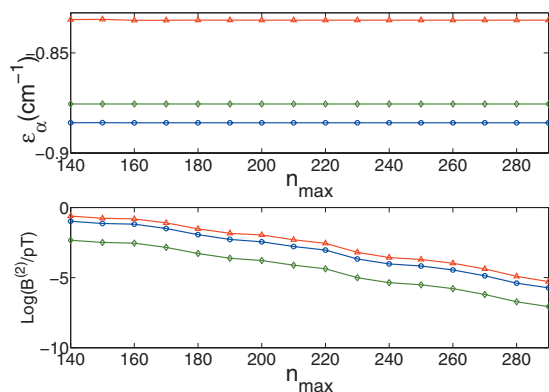
FIG. 7. Lower panel gives the logarithm of the error bounds for three Floquet eigenstates of K, Eq. (7), for $\sigma=0.02$, $T=2$ (both in $\hbar/B$ units), $\Delta\omega=50$, and $J_{max}=40$, as a function of the n_{max} value to which the matrix representation of K is truncated. The upper panel shows the corresponding quasienergies. The lines connect the different points according to quasienergy ordering and they are plotted only to guide the eye but have no other meaning. The same color is used in both panels to identify a given quasienergy and its error bound.

FIG. 9. Cyclic vectors, at $t=-T/2$, for the same parameter values as in Fig. 8. Here $n_{max}=100$ and columns (a) $J_{max}=84$, (b) $J_{max}=86$, and (c) $J_{max}=88$. Colors match those used in Fig. 8.

strong laser intensity, $\Delta\omega=2000$. Here the coupling between $|J\rangle$ states is much larger than in the previous cases but only a small $|n\rangle$ basis set is needed due to the small duration of the pulses and the small temporal separation between pulses. Quasienergies and their error bounds are given in Fig. 8, as a function of J_{max}, for $n_{max}=100$. The lowest quasienergy (blue curve) does not change with J_{max} at the plot resolution but the error bounds vary substantially as in the previous cases. For $J_{max}=76$ the error bound is greater than 0.1, for $J_{max}=114$ is smaller than 10^{-4} and for the larger J_{max}'s shown in the figure increase again. The lowest quasienergy state in columns (a) and (c) of Fig. 9 is the strongly aligned state of Fig. 1. We see in Fig. 8 that the error bounds of the states in the red, blue, and green curves suddenly increase for $J_{max}=86$. Figure 9 shows that now the lowest quasienergy state (the blue state) is a new state, which has very high J components, and it is almost degenerated with the aligned state (now in green). The error bound of the aligned state is
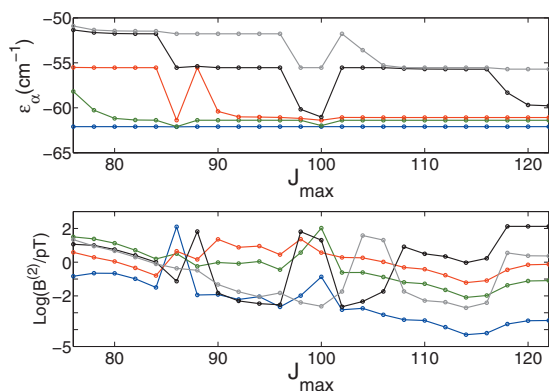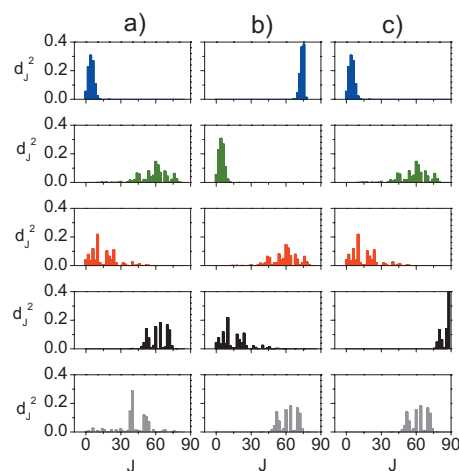
spoiled because it becomes accidentally degenerated with a state which has components near the edge of the matrix and thus, it is a badly converged state. By increasing the number of states in the basis to $J_{max}=88$ the spurious degeneracy disappears and as shown in column (c) of Fig. 9 the aligned state is again the lowest (for the range shown) quasienergy state (in blue) and stays so for $J_{max}=122$. A similar effect appears for $J_{max}=100$ when the aligned state (blue) is degenerated in quasienergy with the red state in column (b) of Fig. 10. Note that the deterioration in the error bound is not as bad as in the previous case because the weight of the highest J component in the red state is less important. It is expected that the overlap between the aligned state and new nonconverged states that could arise for bigger basis sets would be smaller, even at accidental degeneracies, because these new states would be composed of higher J states. We have done a calculation with $J_{max}=260$ and $n_{max}=400$ (the size of the associated Floquet matrix is 104 931) and we got a significant improvement on the error bound, which is now 1.9×10^{-10} for the aligned state shown in Fig. 1 and 1.3×10^{-10} for the misaligned state.
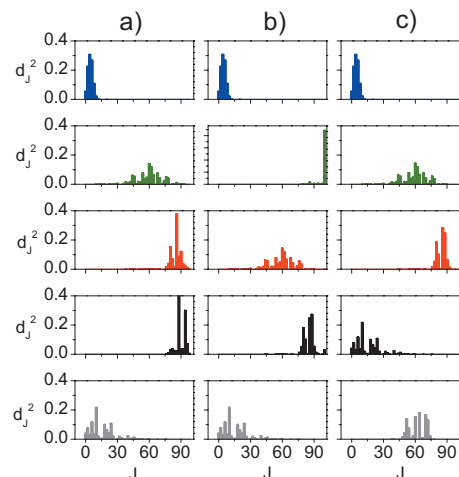

FIG. 8. Lower panel gives the logarithm of the error bounds for five Floquet eigenstates of K, Eq. (7), for $\sigma=0.005$, $T=0.05$ (both in $\hbar/B$ units), $\Delta\omega=2000$, and $n_{max}=100$, as a function of the J_{max} value to which the matrix representation of K is truncated. The upper panel shows the corresponding quasienergies. The lines connect the different points according to quasienergy ordering and they are plotted only to guide the eye but have no other meaning. The same color is used in both panels to identify a given quasienergy and its error bound.

FIG. 10. Cyclic vectors, at $t=-T/2$, for the same parameters as in Fig. 8. Here $n_{max}=100$ and columns (a) $J_{max}=98$, (b) $J_{max}=100$, and (c) $J_{max}=102$. Colors match those used in Fig. 8.

VII. SUMMARY AND CONCLUSIONS

The existence of rotational wave packets for which strong alignment can be maintained during a long sequence of laser pulses was proposed in Ref. 5. These states are eigenstates of the unitary one-period time propagator and were obtained by diagonalizing a finite matrix representation of the Floquet Hamiltonian of the time-dependent system formed by a molecule and a periodic train of nonresonant laser pulses. Since the publication of Ref. 5 we wondered if this behavior could be an artifact caused by the truncation of the infinite Floquet matrix. The reason is that Floquet Hamiltonians of driven systems when the number of states of the field-free Hamiltonian $N \to \infty$ may have no point spectrum, and in that case the eigenpairs of truncated matrices may have nothing to do with generalized eigenpairs of the exact operator.

In Fig. 1 we showed two important characteristics of cyclic aligned rotational wave packets: (i) these states maintain their strong initial alignments after every pulse with small misalignment during each pulse, and (ii) only a few rotational states contribute significantly to strongly aligned wave packets. In Fig. 2 we showed the composition of the two Floquet eigenstates in the extended Hilbert space. In this case, the less aligned state is more extended in J space, but the number of contributing time basis functions is similar in both cases. Figures 3 and 4 show the characteristics of the nonperturbed Floquet operator that make the analysis of the perturbation so difficult, namely, the fact that the spectrum of the field-free Floquet Hamiltonian is pure point but dense when $J \to \infty$ and $n \to \infty$. For finite J_{max} different spectra are obtained depending on the ratio between the rotational frequency and the frequency of repetition of the pulse train.

We applied a theorem by Howland[19] valid for systems for which the field-free Hamiltonian has levels exhibiting increasing gaps and a smooth enough time-dependent perturbation. The theorem proves that the spectrum of the Floquet Hamiltonian for a diatomic molecule, in the $N \to \infty$ limit, driven by nonresonant linearly polarized pulses has no absolutely continuous part. This theorem is based on the adiabatic method and thus the result is valid for any perturbation strength. However, the theorem does not allow us to say if the spectrum is dense pure point or singular continuous. We showed that approximate eigenvectors obtained from truncated matrices cannot be cyclic in the limit $t \to \infty$ if the spectrum is singular continuous. Then, we applied a theorem by Duclos et al.,[20] based on a KAM method and as such only valid for very small perturbations. The theorem indicates that for very weak laser intensities our system has pure point Floquet spectrum for most frequencies except for a set for which it is singular continuous. Unfortunately aligned states do not exist for laser parameters within the range of validity of the theorem, although two propositions of Hone et al.[4] imply that the rigorous results of Duclos et al. should be generally valid for any coupling range.

Finally, we used an expression that gives error bounds for the exact time evolution of a wave function by establishing a comparison with an approximate evolution, which is exactly known. Thus, the error bound gives the norm of the difference between the evolution of the unknown exact wave function and the known approximate wave function. In the regime for which cyclic states are strongly aligned, and for typical experimental conditions regarding duration of the lasers, spacings between pulses, and peak intensities, we obtained that the error bound, for one period, is usually less than 10^{-11}. This implies that the exact wave function behaves quasiciclically for at least 10^9 pulses, and we can state that cyclic wave packets for which strong alignment can be maintained for arbitrarily long times do exist. The reader should take into account that for realistic systems dissipation will destroy alignment in a shorter time. This is not a rigorous proof of the pure point character of the Floquet spectrum but we can safely state that under usual experimental conditions the spectrum of the Floquet Hamiltonian of a molecule interacting with a train of nonresonant laser pulses behaves as if it were pure point.

Quantum dynamics of microscopic systems driven by time-dependent periodic systems has a long history with a key role reserved to the study of the spectrum of the pertinent Floquet Hamiltonian. Most studies were concerned with the analysis of models in the fields of condensed matter physics and quantum chaos with a gradual spread of interest in the last two decades to time-dependent phenomena in atomic physics. Nowadays the interest is moving to molecular systems for which new approaches aimed to get real quantum control of molecules are being developed. This field is being developed by atomic physicists who have an ample expertise in laser techniques and time-dependent calculations and chemical physicists who have a good knowledge of molecular spectroscopy and effective Hamiltonians but that are unfamiliar with the tools that have been developed in the last decades by mathematicians to investigate intricate questions concerning the perturbation of the spectra of unbounded operators. It is hoped that the present paper could help to stimulate the connection between these various fields.

APPENDIX: TWO THEOREMS ON THE SPECTRA OF FLOQUET HAMILTONIANS

Theorem 1: (Howland[19]) Let H_0 be a self-adjoint operator positive and discrete with eigenvalues of simple multiplicity satisfying $\Delta \epsilon = \epsilon_n - \epsilon_{n-1} \geq Cn^\kappa$. Let $V(t) \in C^r$ [i.e., $\max_{l=1,2,\ldots,r} \sup_{t \in R} \|(d/dt)^l V(t)\| < \infty, r < \infty$]. If $r \geq [\kappa^{-1}] + 1$, where $[\cdot]$ stands for the integer part, the Floquet Hamiltonian $K = H_0 + V(t) - \iota \partial/\partial t$ has no absolutely continuous part.

The original formulation of this theorem requires strong differentiability of $V(t)$ [$\lim_{t \to t_0}(d/dt)^l V(t)\chi \to (d/dt)^l V(t)|_{t=t_0}\chi$ $\forall t_0$] but here, to avoid mathematical

subtleties, we follow Nenciu[50] who requires norm differentiability of $V(t)$, with the operator norm defined as $\|(d/dt)^l V(t)\| := \sup_{\|\phi\|=\|\psi\|=1} |\langle \psi, (d/dt)^l V(t)\phi\rangle|$.

Let see now that conditions in the theorem hold for the Floquet Hamiltonian equation (7). Energy levels of $H_0 = \mathbf{J}^2$ are given by $J(J+1)$ (in $B/\hbar$ units). The perturbation $V(t') := -(\Delta\omega\cos^2\theta + \omega_\perp)\exp(-t'^2/\sigma^2)$ only mixes levels with $\Delta J = \pm 2$, therefore H_0 can be divided into two noninteracting blocks, one for J even and the other for J odd. Thus, the gap between two successive (and interacting) eigenvalues is $\Delta\epsilon_J = 4J+6$. Obviously $\Delta\epsilon_J \geq CJ^\kappa$ if $C=4$, $\kappa=1$. Thus, if the periodic perturbation is $V(t) \in C^2$ the conditions in the theorem are obeyed, provided the eigenvalues are nondegenerate. However, rotational levels are $2J+1$ times degenerate, but different M sublevels are not mixed if the external field is linearly polarized. In other words, the Hilbert space is "divided" into $2J+1$ independent subspaces, one for each M value. The theorem applies to each one of the corresponding Hamiltonians if $V(t)$ is two-times norm differentiable with continuous second derivative. Taking into account that the perturbation can be factorized as $V(t) = -\Delta\omega f(t)V(\theta)$, where $V(\theta) = \cos^2\theta$, discarding $\omega_\perp$ in Eq. (7), and using the following expressions for the matrix elements of $\cos^2\theta$ (particularized for $M=0$):[55]

$$\langle J|\cos^2\theta|J+2\rangle = \left[\frac{(J+2)^2(J+1)^2}{(2J+3)^2(2J+5)(2J+1)}\right]^{1/2}, \quad (A1)$$

$$\langle J|\cos^2\theta|J-2\rangle = \left[\frac{J^2(J-1)^2}{(2J-1)^2(2J+1)(2J-3)}\right]^{1/2}, \quad (A2)$$

$$\langle J|\cos^2\theta|J\rangle = \frac{1}{3} + \frac{2}{3}\left[\frac{J(J+1)}{(2J+3)(2J-1)}\right], \quad (A3)$$

$$\langle J|\cos^2\theta|J'\rangle = 0 \quad \text{for} |J'-J| \neq 0, \pm 2, \quad (A4)$$

we get

$$\left\|\frac{d^l V(t)}{dt^l}\right\| = \sup_{\|J\|=\|J'\|=1}|\langle J|\cos^2\theta|J'\rangle|\left|\frac{d^l f(t)}{dt^l}\right|. \quad (A5)$$

For a linearly polarized Gaussian pulse centered at $t_0 = 0$, $f(t) = e^{-t^2/\sigma^2}$, the time derivatives are

$$\frac{df(t)}{dt} = -\frac{2}{\sigma^2}te^{-t^2/\sigma^2}, \quad (A6)$$

$$\frac{d^2 f(t)}{dt^2} = \frac{2}{\sigma^2}\left(\frac{2t^2}{\sigma^2}-1\right)e^{-t^2/\sigma^2}. \quad (A7)$$

Therefore,

$$\sup_{t\in R}\left\|\frac{dV(t)}{dt}\right\| = \frac{3\sqrt{2}\Delta\omega}{5\sqrt{e}\sigma} \quad (A8)$$

and

$$\sup_{t\in R}\left\|\frac{d^2 V(t)}{dt^2}\right\| = \frac{12\Delta\omega}{5e^{3/2}\sigma^2}, \quad (A9)$$

and thus $V(t)$ is at least C^2.

Theorem 2: (Duclos *et al.*[20]) Fix $S>0$ and set

$\Omega_0 := \left[\frac{8}{9}S, \frac{9}{8}S\right]$. Assume that there is a $\gamma>0$, such that

$$\Delta_\gamma^S := S^\gamma \sum_{J,J'} \frac{1}{[J(J+1)-J'(J'+1)]^\gamma} < \infty. \quad (A10)$$

Then, for $r > \gamma+1/2$ there exist positive constants δ_* and ϵ_* with the property: if

$$\epsilon_V := \sup_J \sum_k \sum_{J'} |V_{kJJ'}| \times \max\{|k|^r, 1\} < \min(\epsilon_*, \Omega_0/\delta_*), \quad (A11)$$

then there exists a subset $|\Omega_\infty| \geq |\Omega_0| - \delta_*\epsilon_V$, for which the Floquet Hamiltonian has pure point spectrum for all $\omega(=2\pi/T) \in \Omega_\infty$.

The parameters δ_* and ϵ_* are defined as

$$\delta_* = 1440e^5 2^\gamma \left(\frac{2\gamma+1}{(1-e^{-2/r})e}\right)^{\gamma+1/2}\left(\sum_{s=1}^\infty s^2 e^{-2(r-\gamma-1/2)s/r}\right)\Delta_\gamma^K, \quad (A12)$$

$$\epsilon_* = \min\left\{\frac{2}{135e^3}\inf_J|(J+2)(J+3)-J(J+1)|, \frac{1}{270e^3}K\right\}, \quad (A13)$$

and $V_{kJJ'}$ is the Fourier coefficient of the time-dependent part of the perturbation times the spatial matrix element,

$$V_{kJJ'} := \int_{-T/2}^{T/2} -\Delta\omega f(t)e^{-2\pi\iota kt/T}\langle J,M|\cos^2\theta|J'M\rangle dt. \quad (A14)$$

For the theorem to be applicable ϵ_V in Eq. (A11) must be finite for $r > \gamma+1/2$. Taking into account that $\Delta_\gamma^S < \infty$ for $\gamma \geq 2$ (for example, for $\gamma=2$, $\Delta_2^S = 0.047\,080\,3S^2$), ϵ_V must be finite for $r > 5/2$. We need the following integral for evaluating ϵ_V:

$$z_k(t) := \int_{-T/2}^{T/2} e^{-2\pi\iota kt/T}e^{-t^2/\sigma^2}dt$$

$$= \left(\frac{\sqrt{\pi}\sigma\iota}{2T}\right)e^{-(k\pi\sigma/T)^2}\left[\text{Erfi}\left(\frac{k\pi\sigma}{T}-\frac{\iota T}{2\sigma}\right)\right.$$

$$\left. - \text{Erfi}\left(\frac{k\pi\sigma}{T}+\frac{\iota T}{2\sigma}\right)\right], \quad (A15)$$

with $k=n-m$, and $\text{Erfi}[z] = -(2\iota/\sqrt{\pi})\int_0^{\iota z}e^{-t^2}dt$ the imaginary error function.[56] For a laser pulse with $T \gg \sigma$ the following approximation for z_k allows us an easier evaluation of the infinite sum arising in the definition of ϵ_V:

$$z_k = \frac{\sqrt{\pi}\sigma}{T}\exp(-(\pi\sigma k/T)^2). \quad (A16)$$

Thus, we get the following expression for ϵ_V:

$$\epsilon_V = \sup_J \sum_k \frac{\Delta\omega\sqrt{\pi}\sigma}{T} \exp(-(\pi\sigma k/T)^2)$$

$$\times \left\{ \left[\frac{(J+2)^2(J+1)^2}{(2J+3)^2(2J+5)(2J+1)} \right]^{1/2} \right.$$

$$+ \left[\frac{J^2(J-1)^2}{(2J-1)^2(2J+1)(2J-3)} \right]^{1/2} + \frac{1}{3}$$

$$\left. + \frac{2}{3} \left[\frac{J(J+1)}{(2J+3)(2J-1)} \right] \right\} \times \max\{|k|^r, 1\}. \qquad \text{(A17)}$$

For a pulse with $\sigma = 0.1$, $T = 1$, and choosing $r = 3$, we get $\Sigma_k |z_k| \max(|k|^3, 1) = 18.3763 \Delta\omega$ and $\epsilon_V = 19.8 \Delta\omega$. Thus, the spectrum of the Floquet Hamiltonian will be pure point for a subset $|\Omega_\infty|$ if $\Delta\omega < \min(\epsilon_*, |\Omega_0|/\delta_*)/19.8$. For the chosen period of the laser field, we can take $S = 2\pi$. By substituting this S value in the estimates $\epsilon_* = 1.8 \times 10^{-4} S$ and $\delta_* = 6.0 \times 10^7 S^2$, Theorem 2 implies that the spectrum of the Floquet Hamiltonian is pure point for a subset of $\omega's$, $|\Omega_\infty|$ if $\Delta\omega < 3 \times 10^{-11}$. The corresponding laser intensity can be obtained from Eq. (8).

[1] I. Bloch, J. Dalibard, and W. Zwerger, Rev. Mod. Phys. **80**, 885 (2008).
[2] H. H. Fielding, Annu. Rev. Phys. Chem. **56**, 91 (2005).
[3] H. Stapelfeldt and T. Seideman, Rev. Mod. Phys. **75**, 543 (2003).
[4] D. W. Hone, W. Ketzmerick, and W. Kohn, Phys. Rev. A **56**, 4045 (1997).
[5] J. Ortigoso, Phys. Rev. Lett. **93**, 073001 (2004).
[6] J. Ortigoso and J. Santos, Phys. Rev. A **72**, 053401 (2005).
[7] D. R. Hofstadter, Phys. Rev. B **14**, 2239 (1976).
[8] G. Casati, J. Ford, I. Guarneri, and F. Vivaldi, Phys. Rev. A **34**, 1413 (1986).
[9] N. Goldman, J. Phys. B **42**, 055302 (2009).
[10] J. S. Howland, Lect. Notes Phys. **403**, 100 (1992).
[11] B. V. Chirikov, Phys. Rep. **52**, 263 (1979).
[12] B. Dorizzi, B. Grammaticos, and Y. Pomeau, J. Stat. Phys. **37**, 93 (1984).
[13] H. J. Korsch, E. M. Graefe, and H.-J. Jodl, Am. J. Phys. **76**, 498 (2008).
[14] S. Fishman, in Proceedings of the International School of Physics "Enrico Fermi," Varenna, July 1991, edited by G. Casati, I. Guarneri, and U. Smilansky (North-Holland, New York, 1993).
[15] R. Blümel, S. Fishman, and U. Smilansky, J. Chem. Phys. **84**, 2604 (1986); S. Fishman, Phys. Scr. **40**, 416 (1989).
[16] M. Feingold, S. Fishman, D. R. Grempel, and R. E. Prange, Phys. Rev. B **31**, 6852 (1985).
[17] T. Seideman, J. Chem. Phys. **103**, 7887 (1995); Phys. Rev. Lett. **83**, 4971 (1999).
[18] A. Pelzer, S. Ramakrishna, and T. Seideman, J. Chem. Phys. **126**, 034503 (2007); C. Buth and R. Santra, ibid. **129**, 134312 (2008).
[19] J. S. Howland, Ann. Inst. Henri Poincare, Sect. A **50**, 325 (1989).
[20] P. Duclos, O. Lev, P. Štovíček, and M. Vittot, Rev. Math. Phys. **14**, 531 (2002).
[21] J. H. Shirley, Phys. Rev. **138**, B979 (1965).
[22] H. Sambe, Phys. Rev. A **7**, 2203 (1973).
[23] J. S. Howland, Math. Ann. **207**, 315 (1974); Indiana Univ. Math. J. **28**, 471 (1979).
[24] K. Yajima, J. Math. Soc. Jpn. **29**, 729 (1977).
[25] P. Pfeifer and R. D. Levine, J. Chem. Phys. **79**, 5512 (1983).
[26] U. Peskin and N. Moiseyev, J. Chem. Phys. **99**, 4590 (1993).
[27] N. Moiseyev, Comments At. Mol. Phys. **31**, 87 (1995).
[28] G. Jolicard and J. P. Killingbeck, J. Phys. A **36**, R411 (2003).
[29] A. Buchleitner, D. Delande, and Z. Zakrzewski, Phys. Rep. **368**, 409 (2002).
[30] B. Friedrich and D. Herschbach, Phys. Rev. Lett. **74**, 4623 (1995).
[31] J. Ortigoso, M. Rodríguez, M. Gupta, and B. Friedrich, J. Chem. Phys. **110**, 3870 (1999).
[32] B. Friedrich and D. Herschbach, J. Phys. Chem. **99**, 15686 (1995).
[33] U. Peskin and N. Moiseyev, Phys. Rev. A **49**, 3712 (1994).
[34] J. Ortigoso, Phys. Rev. A **70**, 055401 (2004).
[35] C. R. de Oliveira, Mathematical Physics (Birkhauser, Basel, 2009), Vol. 54.
[36] D. R. Grempel, R. E. Prange, and S. Fishman, Phys. Rev. A **29**, 1639 (1984).
[37] J. B. Sokoloff, Phys. Rep. **126**, 189 (1985).
[38] T. Geisel, R. Ketzmerick, and G. Petschel, Phys. Rev. Lett. **67**, 3635 (1991).
[39] P. Duclos, P. Štovíček, and M. Vittot, Ann. Inst. Henri Poincare, Sect. A **71**, 241 (1999).
[40] J. Bellisard, in Stability and Instability in Quantum Mechanics in Trends and Developments in the Eighties, edited by S. Albeverio and P. Blanchard (Word Scientific, Singapore, 1985).
[41] R. H. Young, W. J. Deal, Jr., and N. R. Kestner, Mol. Phys. **17**, 369 (1969).
[42] T. Hogg and B. A. Huberman, Phys. Rev. Lett. **48**, 711 (1982); Phys. Rev. A **28**, 22 (1983).
[43] Y. Last, J. Funct. Anal. **142**, 406 (1996).
[44] R. E. Prange, D. R. Grempel, and S. Fishman, Phys. Rev. B **28**, 7370 (1983); **29**, 6500 (1984).
[45] K. Yajima and H. Kitada, Ann. Inst. Henri Poincare, Sect. A **39**, 145 (1983).
[46] C. R. de Oliveira, J. Stat. Phys. **78**, 1055 (1995).
[47] R. W. Carey and J. D. Pincus, Am. J. Math. **98**, 481 (1976).
[48] J. S. Howland, Ann. Inst. Henri Poincare, Sect. A **50**, 309 (1989).
[49] A. Joye, J. Stat. Phys. **75**, 929 (1994).
[50] G. Nenciu, Ann. Inst. Henri Poincare, Sect. A **67**, 411 (1997).
[51] R. H. Young and W. J. Deal, Jr., Phys. Rev. A **1**, 419 (1970); J. Math. Phys. **11**, 3298 (1970).
[52] P. Pfeifer and J. Fröhlich, Rev. Mod. Phys. **67**, 759 (1995).
[53] M. Uhlmann, T. Kunert, and R. Schmidt, Phys. Rev. E **72**, 036704 (2005).
[54] J. B. Lehouck, K. Maschhoff, D. Sorensen, and C. Yang, ARPACK software package, http://www.caam.rice.edu/software/ARPACK.
[55] A. Ben Haj-Yedder, A. Auger, C. M. Dion, E. Cancès, A. Keller, C. Le Bris, and O. Atabek, Phys. Rev. A **66**, 063401 (2002).
[56] M. Abramowitz and I. A. Stegun, Handbook of Mathematical Functions (Dover, New York, 1972).